Electronic Supplementary Material (ESI) for Journal of Materials Chemistry A.


# Supporting Information

## Nickel Nitride as an Efficient Electrocatalyst for Water Splitting

*Menny Shalom*, Debora Ressnig, Xiaofei Yang, Guylhaine Clavel, Tim-Patrick Fellinger and Markus Antonietti*

Max Planck Institute of Colloids and Interfaces, Department of Colloid Chemistry, Research Campus Golm, 14424 Postdam, Germany

E-mail address: menny.shalom@mpikg.mpg.de

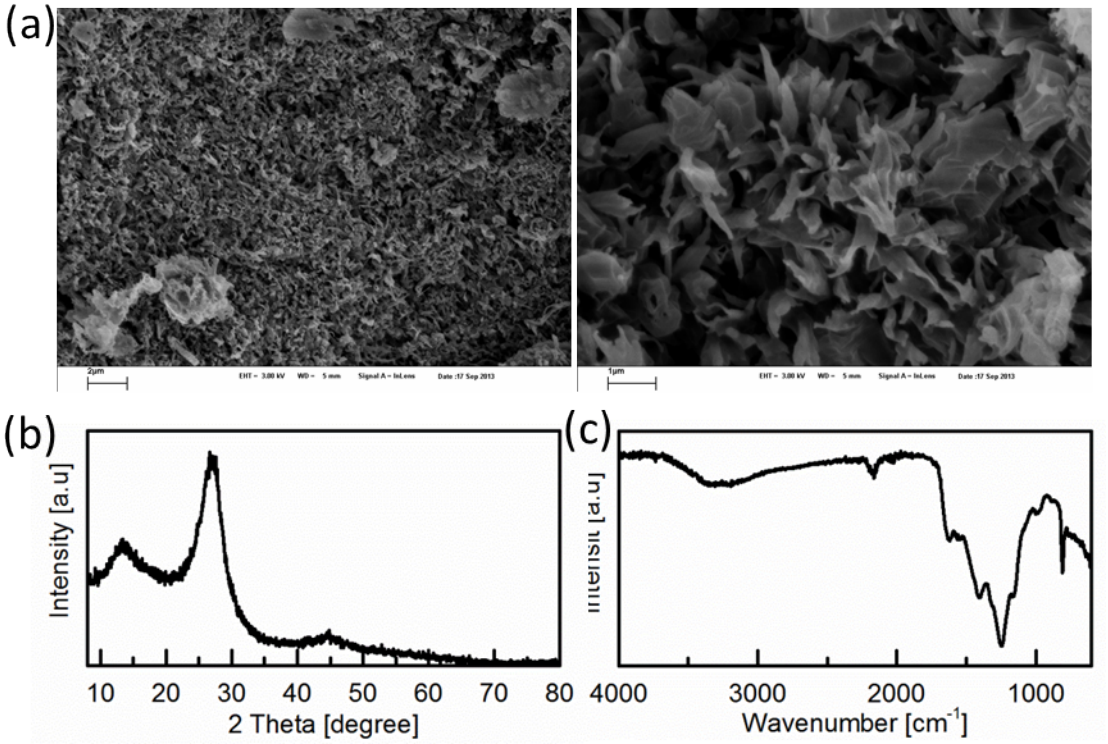


**Figure S1.** SEM images (a) XRD pattern (b) and FTIR spectrum (c) of the carbon-nitride-like material formed on the Ni-foam.

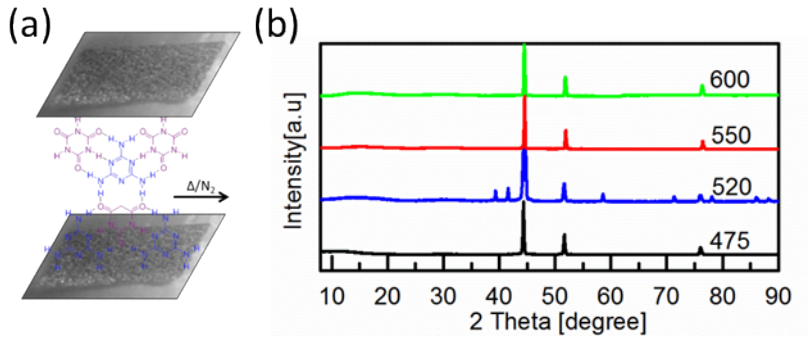


**Figure S2.** Illustration of the CMB complex on Ni-foam (a) and the X-ray diffraction patterns of the Ni-foam modified at different temperatures (b).

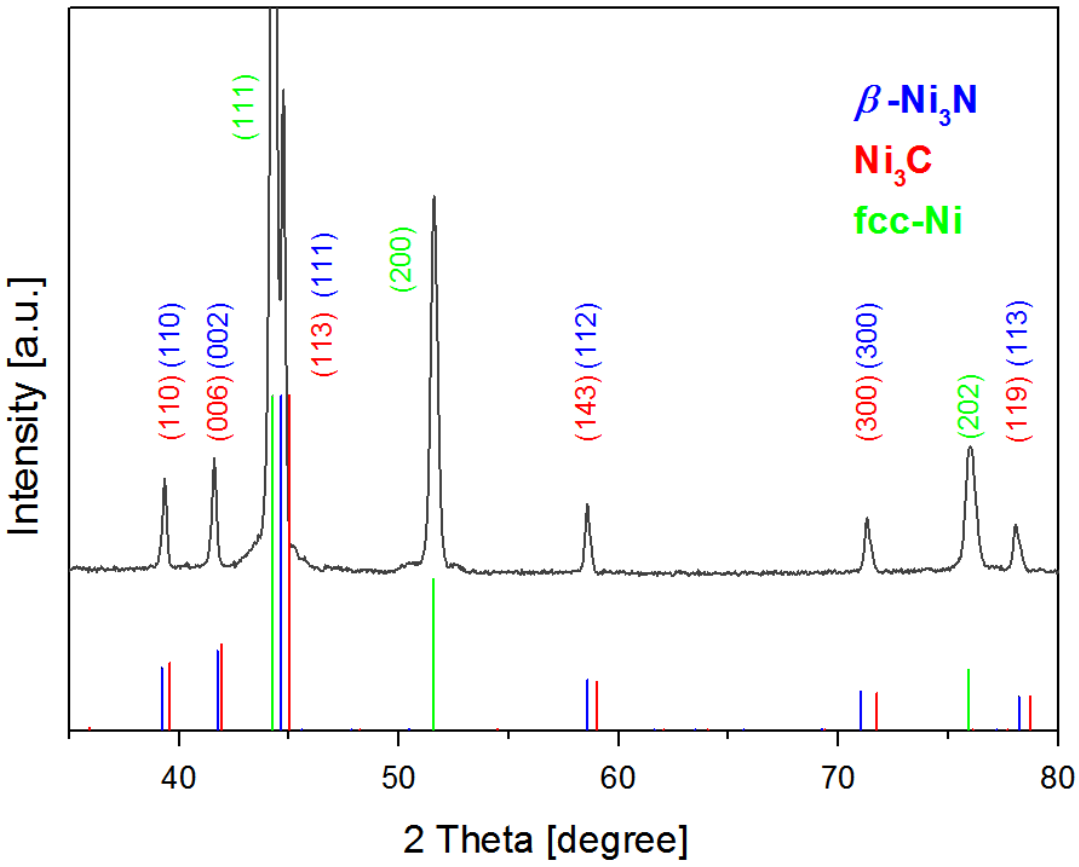


**Figure S3.** The X-ray diffraction pattern of a Ni/$Ni_3N$-foam is shown together with reference patterns of $Ni_3N$ [ICDD 04-011-7280], $Ni_3C$ [ICDD 04-007-3753] and fcc-Ni [ICDD 04-016-4592]. The experimental reflections correlate better with the reference pattern of hexagonal *β*-$Ni_3N$ than with the rhombohedral $Ni_3C$. It is very likely that carbon impurities present in the *β*-$Ni_3N$ host lattice cause the observed shift of the reflections compared to the reference ones. Structure-composition relationships of $Ni_3X$ phases as well as of hcp-Ni are still under intensive debate. Allotropes of hcp-Ni have been reported but experimental conditions and follow up studies strongly suggest that, in most cases, the metastable phase is in fact stabilized with small amounts of impurity elements (H, C, N). The crystallographic information therefore gives insights on spatial and geometric restructuration of the Ni-foam during the synthesis, where the closed packed fcc-Ni structure is opened up with impurity elements. (see also Figure S15).

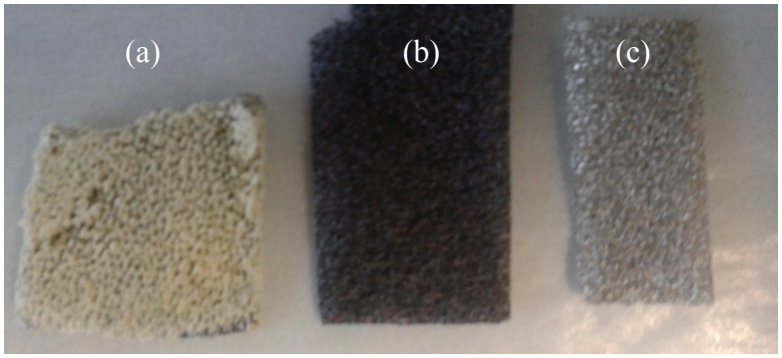


**Figure S4.** Photograph of Ni-foams modified with melamine (a) and CMB (b) precursor complexes in comparison to the pristine foam (c).

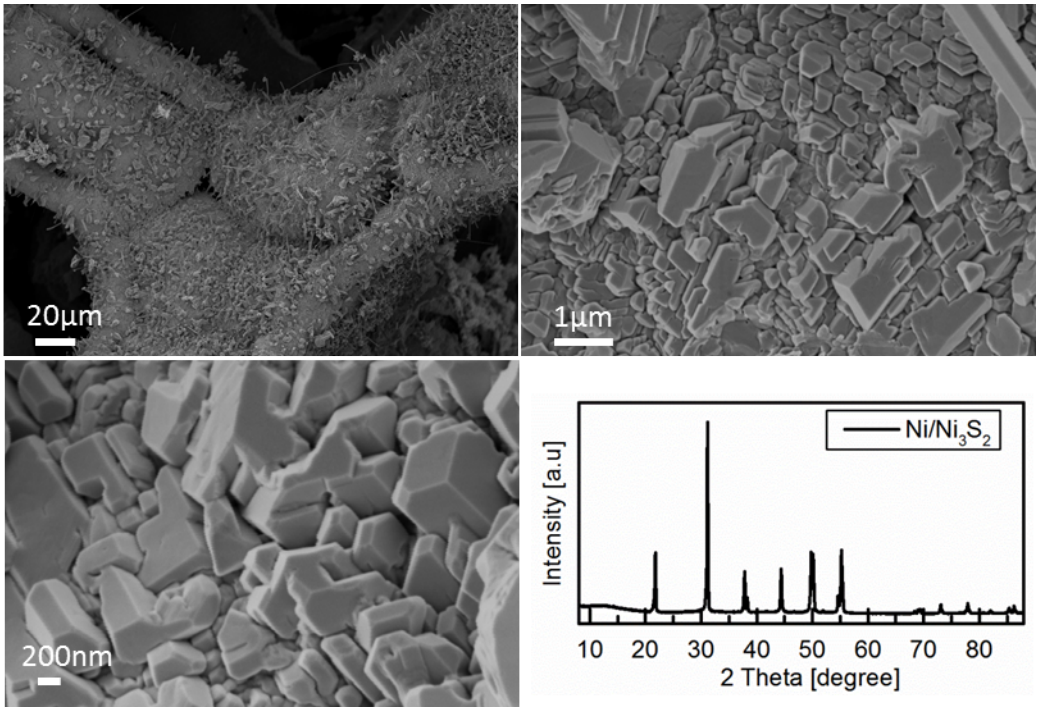


**Figure S5.** SEM images and XRD pattern of a Ni-foam modified with the cyanuric acid-trithiocyanuric acid complex and the corresponding PXRD pattern of $Ni_3S_2$ (ref 04-008-8458).

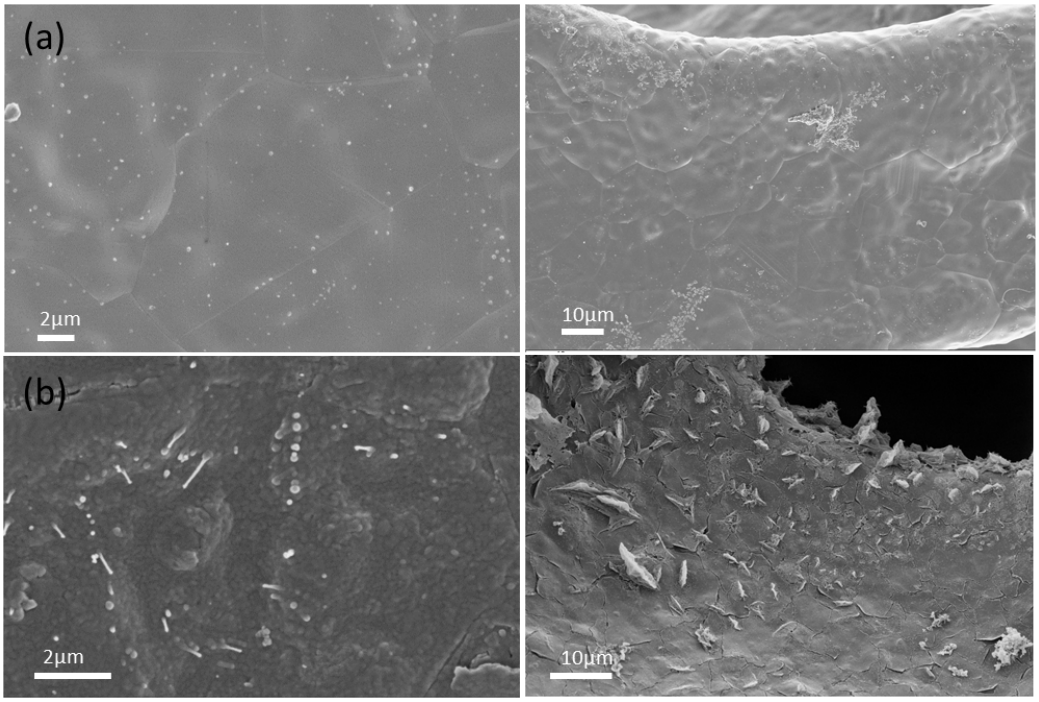


**Figure S6.** SEM images of the original foam (a) compared to the modified foam (b).

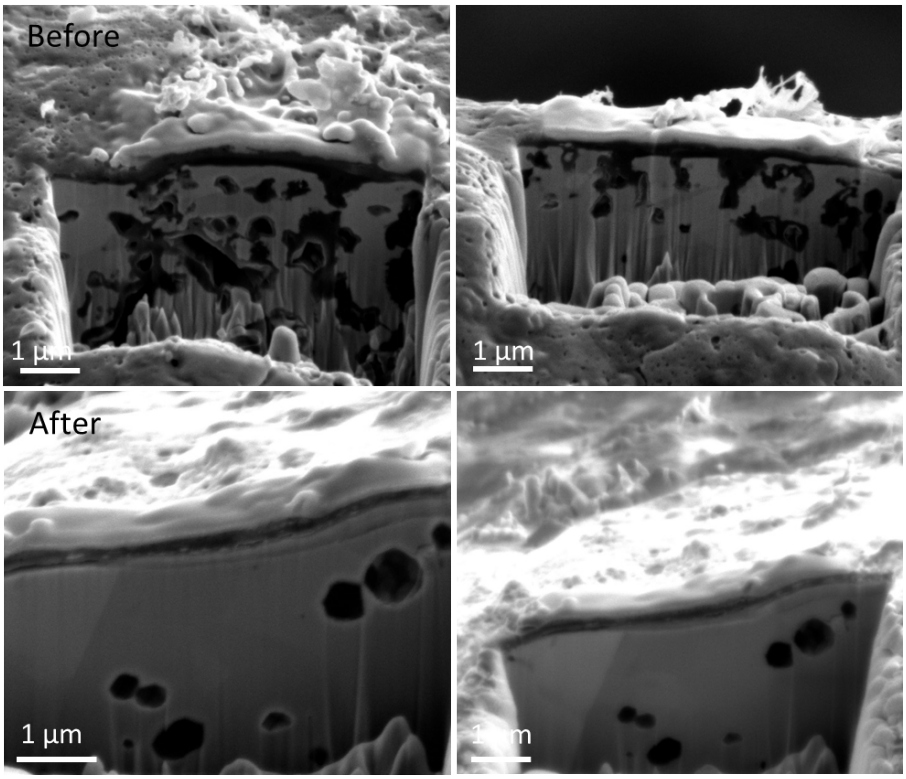


**Figure S7.** SEM images of the modified foam before and after the removal of the carbon-nitride layer with 500 CV cycles (0-0.6V vs. RHE).

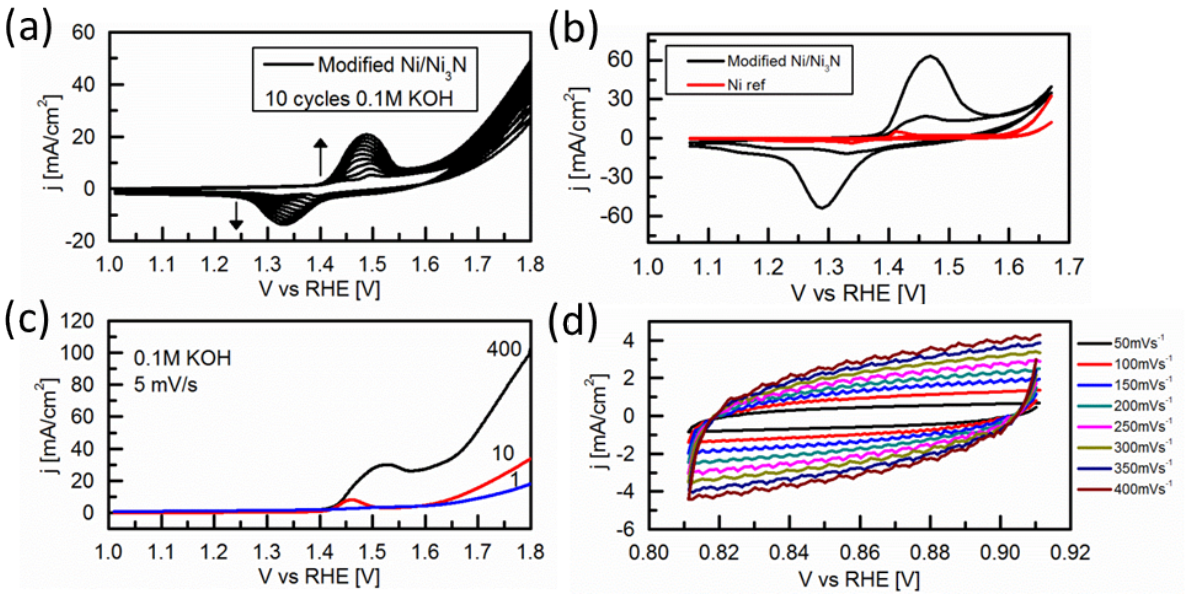


**Figure S8.** (a) First 10 cyclic voltammetry measurements (25 mV/s scan rate, 0.1M KOH) of the modified foam (b) the fifth and the five hundredth cyclic voltammetry measurements of the modified foam compared to the original foam (c) comparison of linear sweep voltammetry (LSV, 1mV/s scan rate) curves for the oxygen evolution reaction before and after 10 and 400 CV cycles and (d) double-layer capacitance measurements for determining the electrochemically active surface area of the modified foam from CV in 1 M KOH.

| Foam | Double-layer capacitance (mF) | R-Square |
|---|---|---|
| Original Ni | -1.89 | 0.99 |
| | 1.73 | 0.991 |
| Modified $Ni/Ni_3N$ | -7.61 | 0.992 |
| | 6.98 | 0.988 |

**Table S1.** Double-layer capacitance data of the modified foam compared to the original one.

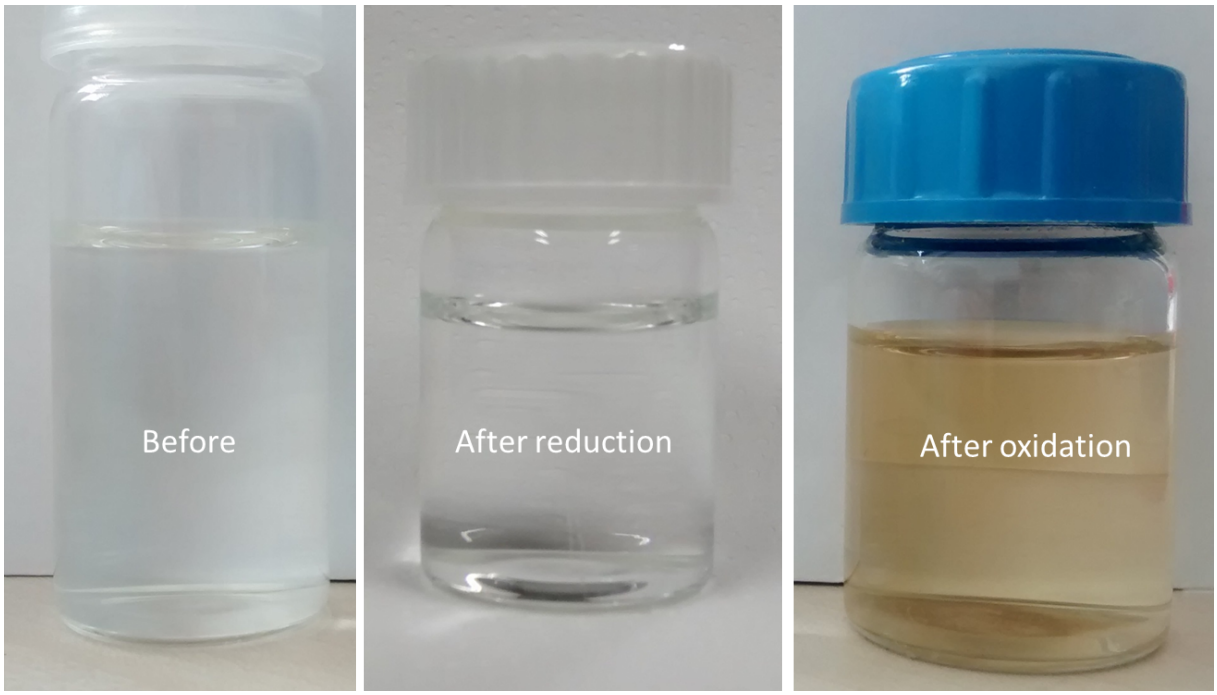


**Figure S9.** 1 M KOH solution before and after the first 500 CV reduction cycles and after 500 CV oxidation cycles. The yellow color is due to the dissolution of the carbon nitride layer (occurs only by oxidation).

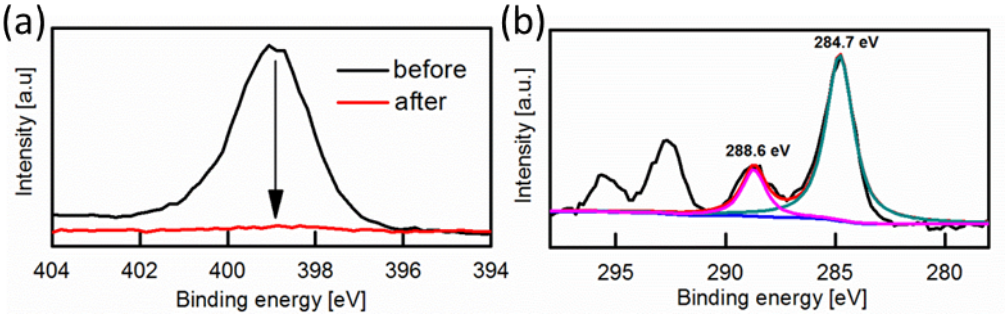


**Figure S10.** High-resolution N1s XPS spectra before and after 500 CV oxidation cycles (a) high-resolution C1s XPS spectra after 500 CV cycles (0-0.6V vs. RHE) (b). The peaks at 293 and 295 eV are attributed to potassium from the KOH solution.

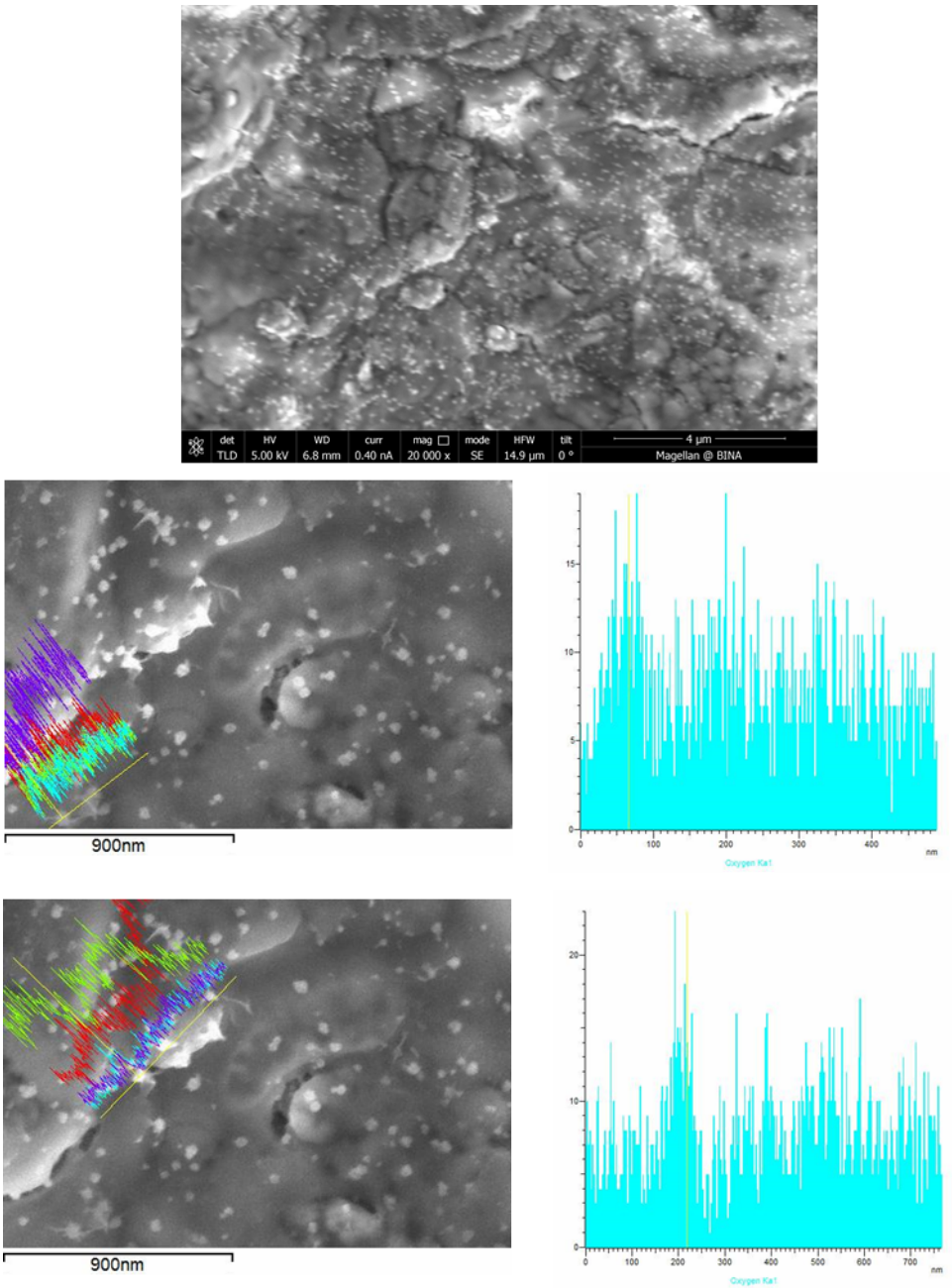


**Figure S11.** SEM images and EDX pattern of two different areas of the modified foam after operation at 500 CV oxidation cycles. The red color is for carbon, green is for nitrogen, purple is for Ni and light blue is for oxygen.

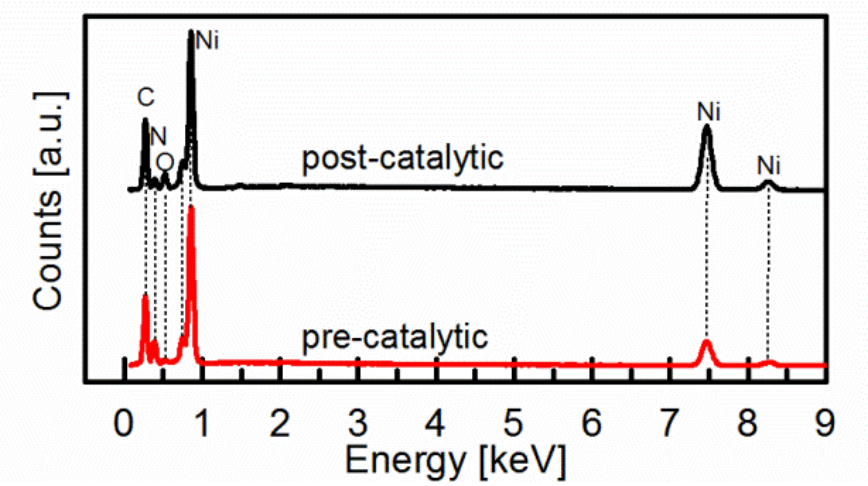


**Figure S12.** Energy-dispersive X-ray (EDX) spectra of the modified Ni-foam before and after activation.

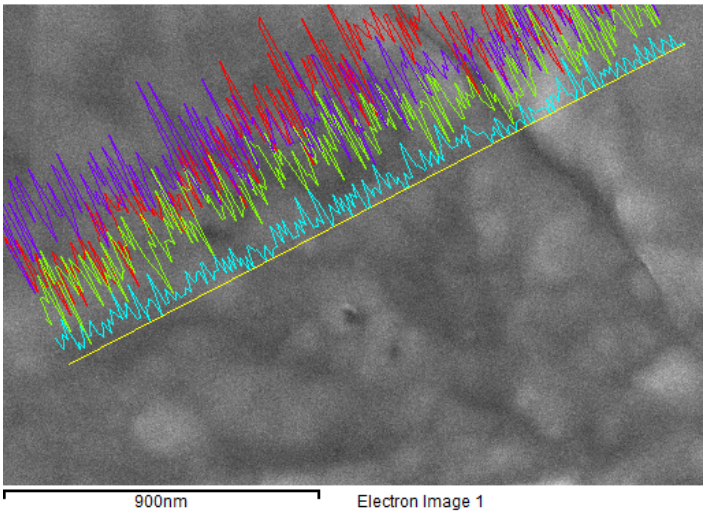


**Figure S13.** SEM images and EDX patterns of the modified foam before operation. The red color corresponds to carbon, green to nitrogen, purple to nickel and light blue to oxygen.

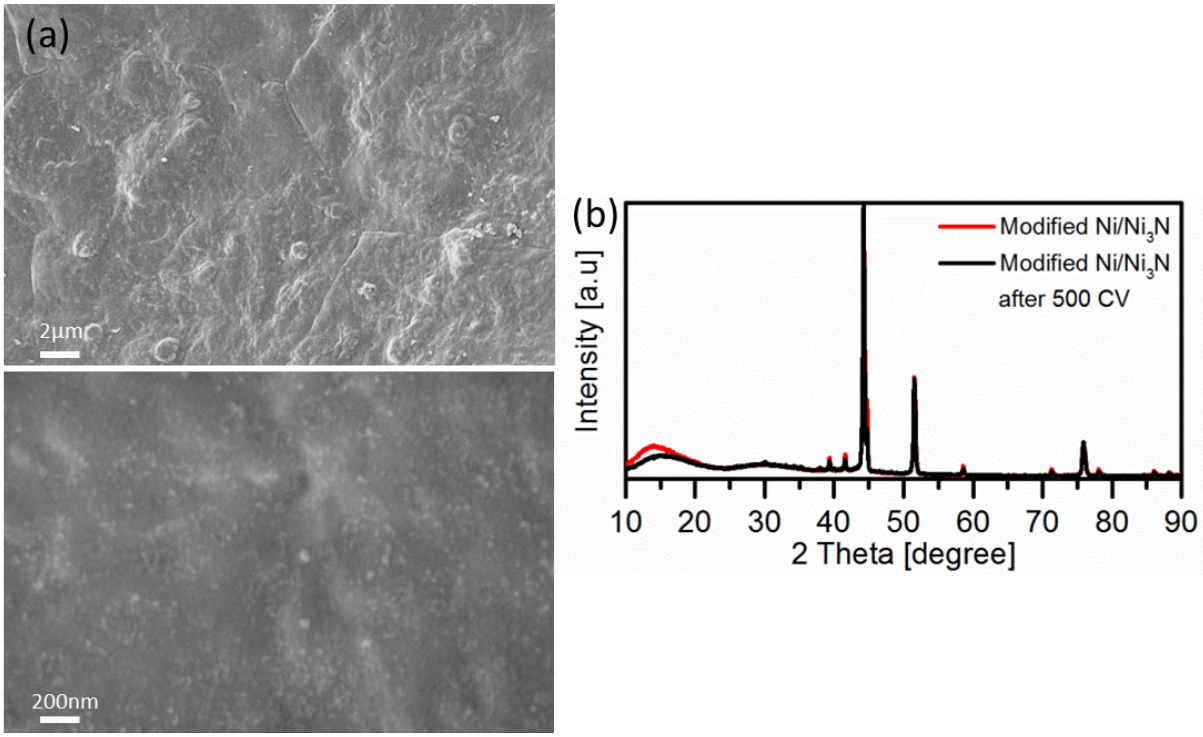


**Figure S14**. SEM images (a) and X-ray diffraction patterns of the modified foam (black) after 500 cyclic voltammetry cycles compare to the modified foam before electrochemical activation (red) (b).

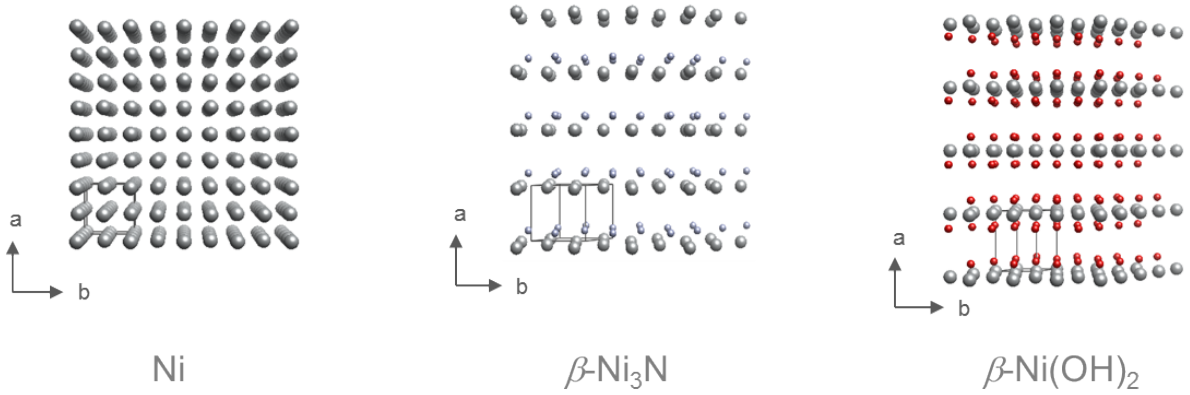


**Figure S15.** Comparison of the atomic packing in cubic-Ni and hexagonal $\beta$-$Ni_3N$ or $\beta$-$Ni(OH)_2$ respectively.

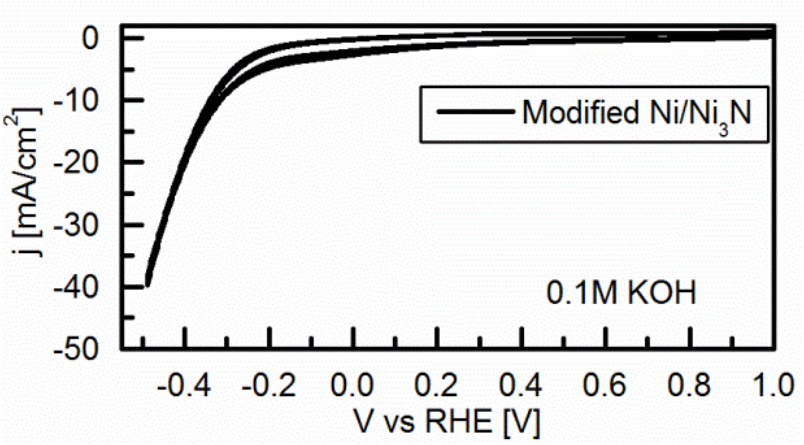


**Figure S16**. Cyclic voltammetry measurements (50 scans, 25mV/s scan rate, 0.1M KOH) of the modified foam before activation.

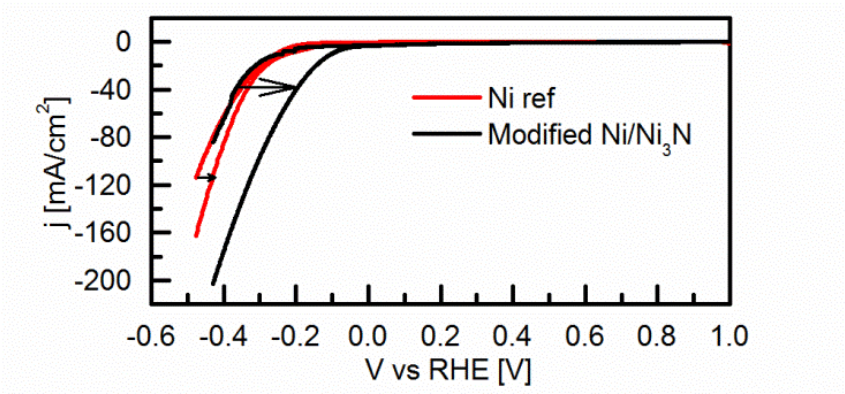


**Figure S17.** Linear sweep voltammetry curves (LSV, 1mV/s scan rate) for the hydrogen evolution reaction with the $Ni/Ni_3N$-foam compared to the original Ni-foam before and after 500 CV oxidation cycles. The arrow shows the changes of the curves before and after the 500 CV oxidation cycles.

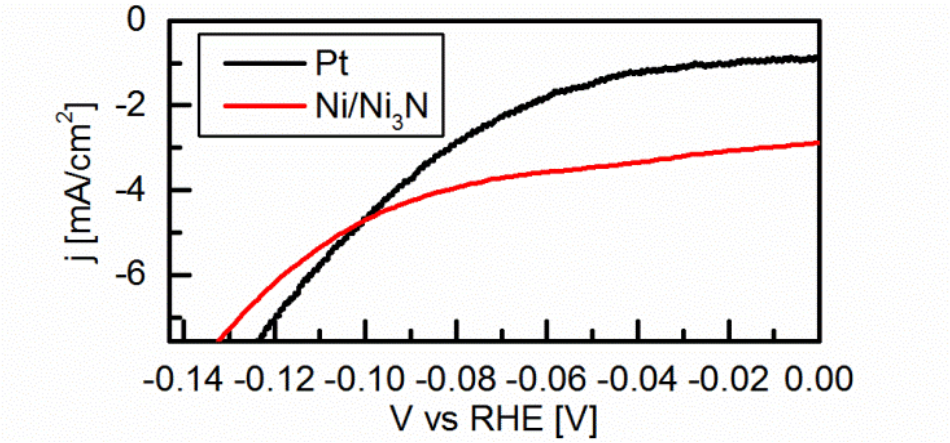


**Figure S18.** Linear sweep voltammetry (LSV, 1mV/s scan rate) for the hydrogen evolution reaction of the $Ni/Ni_3N$-foam compared to a Pt wire.

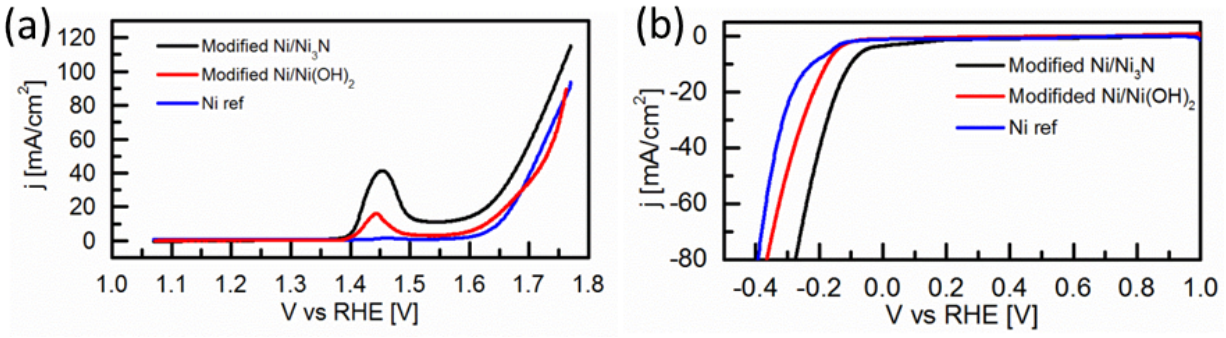


**Figure S19.** Linear sweep voltammetry (LSV, 1mV/s scan rate) for the hydrogen evolution reaction (a) and oxygen evolution reaction of $Ni/Ni_3N$-foam compared to the original Ni-foam and to $Ni/Ni(OH)_2$-foam (b).

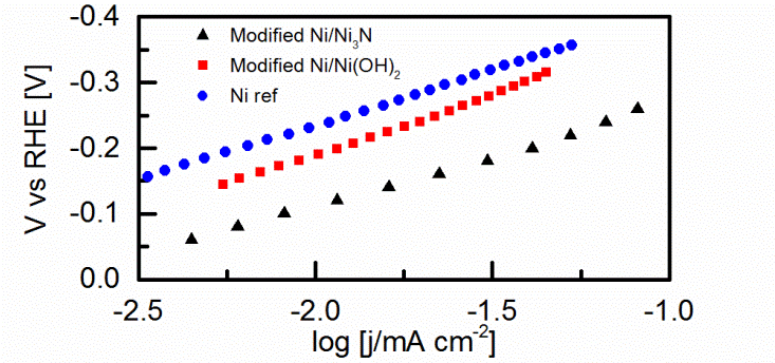


**Figure S20.** Tafel slopes for $Ni/Ni_3N$-foam compared to the original Ni-foam and to the $Ni/Ni(OH)_2$-foam.

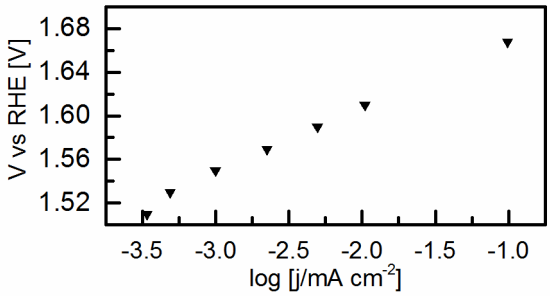


**Figure S21**. Tafel slopes (65 mV $dec^{-1}$) for $Ni/Ni_3N$-foam.

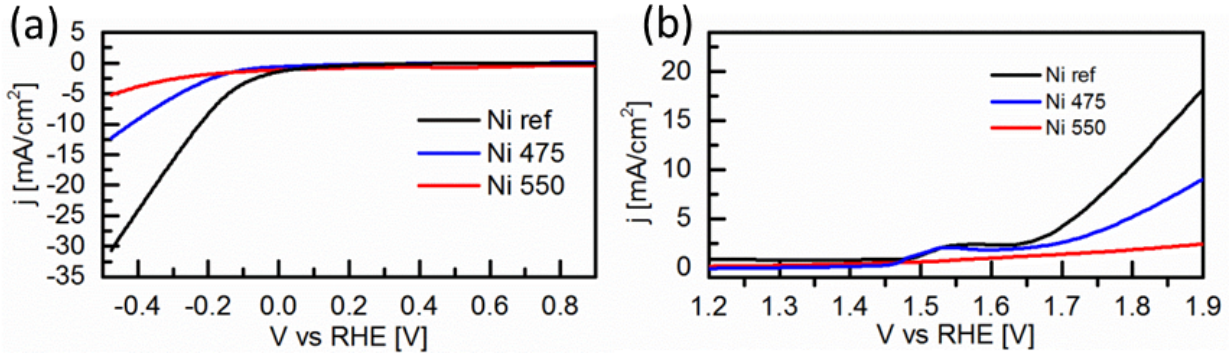


**Figure S22.** Comparison of linear sweeps voltammetry curves (LSV, 1mV/s scan rate, 0.1M KOH) of the modified foam prepared at different temperatures for HER (a) and OER (b).

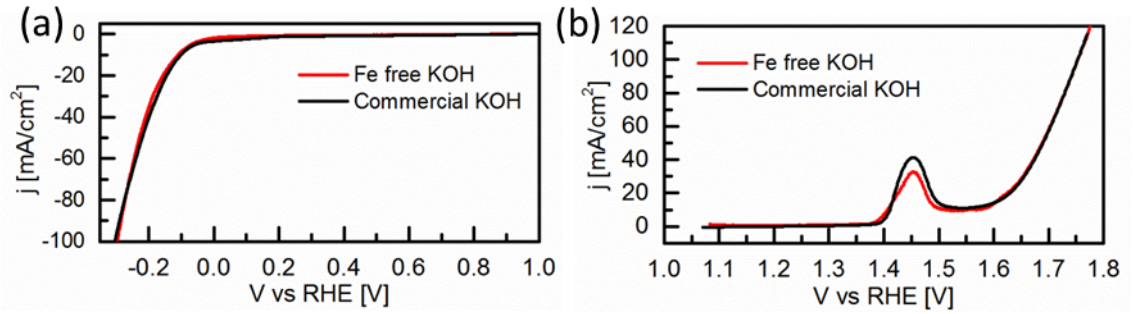


**Figure S23.** Linear sweep voltammetry (LSV, 1mV/s scan rate) for the hydrogen evolution reaction (a) and oxygen evolution reaction of $Ni/Ni_3N$-foam (b) in commercial and purified 1M KOH.

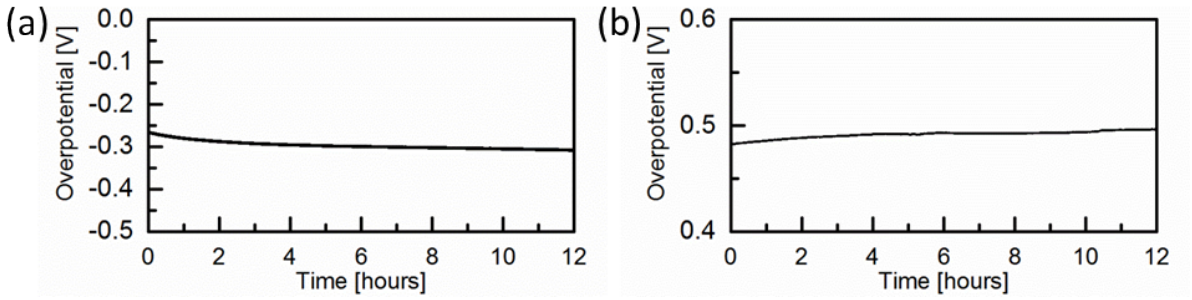


**Figure S24.** Electrolysis at 100 mA $cm^{-2}$ per geometric area for the hydrogen evolution reaction (a) and oxygen evolution reaction of $Ni/Ni_3N$-foam (b) in 1M KOH at 25 °C.

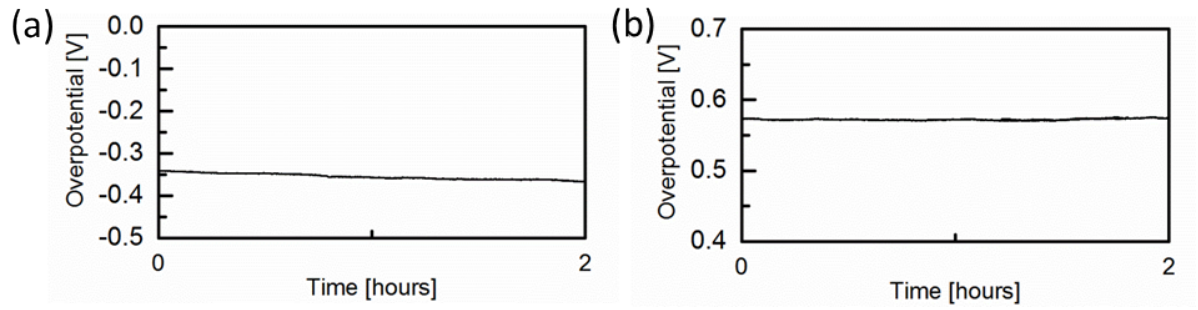


**Figure S25.** Electrolysis at 250 mA $cm^{-2}$ per geometric area for the hydrogen evolution reaction (a) and oxygen evolution reaction of $Ni/Ni_3N$-foam (b) in 1M KOH at 61 °C.

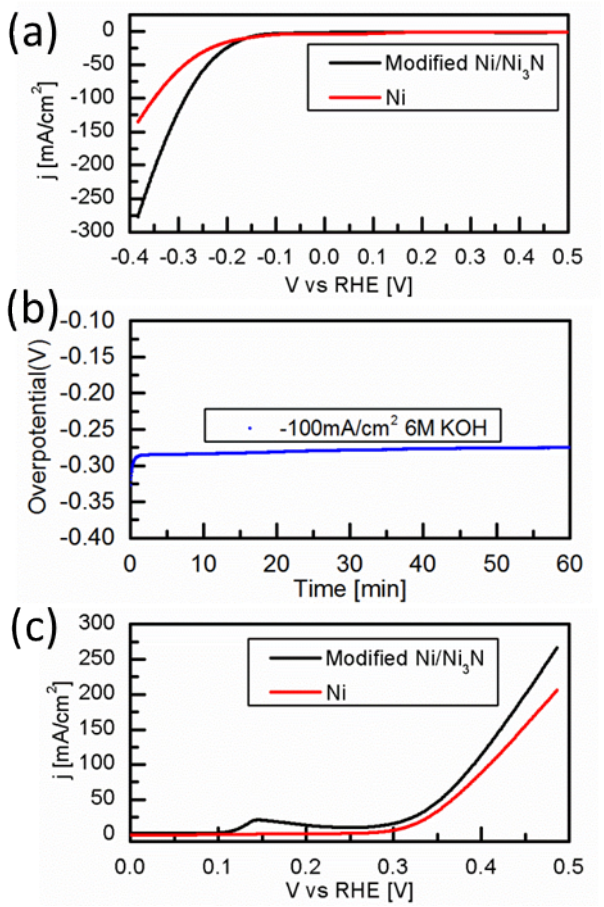


**Figure S26.** Comparison of the linear sweep voltammetry (LSV, 1 mV/s scan rate) curves of the modified foam with respect to the original foam in 6M KOH for (a) HER and(c) OER. Electrolysis (HER) -100 mA $cm^{-2}$ per geometric area of the modified foam for 1h in 6M KOH.